
Article:
Smith, S.A., Colley, H.E., Sharma, P. et al. (5 more authors) (2018) Expression and enzyme activity of Cytochrome P450 enzymes CYP3A4 and CYP3A5 in human skin and tissue engineered skin equivalents. Experimental Dermatology, 27 (5). pp. 473-475. ISSN 0906-6705

https://doi.org/10.1111/exd.13483

Experimental Dermatology ADF

Expression and enzyme activity of Cytochrome P450 enzymes CYP3A4 and CYP3A5 in human skin and tissue engineered skin equivalents

Journal:	*Experimental Dermatology*
Manuscript ID	EXD-17-0151.R1
Manuscript Type:	Letter to the Editors
Date Submitted by the Author:	n/a
Complete List of Authors:	Smith, Sarah; Faculty of Medicine Dentistry and Health Colley, Helen; Faculty of Medicine Dentistry and Health Sharma, Parveen; University of Liverpool, MRC Centre for Drug Safety Science Slowik, Klaudia; Faculty of Medicine Dentistry and Health Sison-Young, Rowena; University of Liverpool, MRC Centre for Drug Safety Science Sneddon, Andrew; Liverpool John Moores University, Department of Applied Mathmatics Webb, Steven; Liverpool John Moores University, Department of Applied Mathmatics Murdoch, Craig; Faculty of Medicine Dentistry and Health
Keywords:	Epithelium, Steroids, Three dimensional tissue models, Xenobiotic metabolism, Toxicity

Expression and enzyme activity of Cytochrome P450 enzymes CYP3A4 and CYP3A5 in human skin and tissue engineered skin equivalents

Sarah A. Smith[1], Helen E. Colley[1*], Parveen Sharma[2], Klaudia M. Slowik[1], Rowena Sison-Young[2], Andrew Sneddon[3], Steven D. Webb[3], Craig Murdoch[1]

[1]School of Clinical Dentistry, University of Sheffield, Claremont Crescent, Sheffield, S10 2TA, UK.

[2]MRC Centre for Drug Safety Science, Department of Molecular and Clinical Pharmacology, Sherrington Building, Ashton Street, University of Liverpool, L69 3GE, UK.

[3]Department of Applied Mathematics, Liverpool John Moores University, James Parsons Building, Byrom Street, Liverpool, L3 3AF, UK.

*Corresponding author: Dr Helen Colley, School of Clinical Dentistry, University of Sheffield, Claremont Crescent, Sheffield, S10 2TA, UK. E-mail. h.colley@sheffield.ac.uk; Tel: +44 114 2259352

Abstract

CYP3A4 and CYP4A5 share specificity for a wide range of xenobiotics with the CYP3 subfamily collectively involved in the biotransformation of approximately 30% of all drugs. CYP3A4/5 mRNA transcripts have been reported in the skin yet knowledge of their protein expression and function is lacking. In this study, we observed gene and protein expression of CYP3A4/5 in both human skin and tissue-engineered skin equivalents (TESE), and enzyme activity was detected using the model substrate benzyl-*O*-methyl-cyanocoumarin. Mass spectrometric analysis of TESE lysates following testosterone application revealed a time-dependent increase in metabolite production, confirming the functional expression of these enzymes in skin.

1 Background

Cytochrome P450 (CYP450) enzymes are a superfamily of hemoproteins that metabolize a multitude of endogenous and xenobiotic molecules and are essential to maintain homeostasis.[1, 2] As the most highly expressed xenobiotic enzymes in the liver, they are responsible for the majority of phase I reactions, metabolizing between 70-80% of all drugs.[3, 4] The CYP3 subfamily of the CYP450 enzymes comprising of CYP3A4, CYP3A5, CYP3A7 and CYP3A43 are, collectively involved in the metabolism of over a third of these drugs.[4] CYP3A4, the most abundantly expressed isoform in the liver,[5] has a large active site that enables its interaction with a wide range of structurally diverse compounds and permits metabolism of such molecules and drugs as hormones (testosterone, estrogen), anti-cancer drugs (paclitaxel, tamoxifen), and anti-fungal agents (ketoconazole) amongst others.[4, 6] CYP3A5 shares 85% amino acid sequence homology with CYP3A4 and displays similar substrate specificity.[7] Gene expression of CYP3A4 and CYP3A5 has been detected in skin and tissue engineered skin equivalents (TESE) by genomic analysis in some studies[8, 9, S1, S2] but not others[S3] and, to date, protein expression has not been detected.[S4, S5] Given the use of skin as a drug delivery route, it is extremely important to determine functional expression of CYP3A4/5. Moreover, the increasing use of TESE as an alternative to animal testing for drug irritation and sensitivity assays has led to their proposed use in drug-induced toxicity assays. However, data on functional xenobiotic enzyme activity in these models is lacking and urgently required.

2 QUESTIONS ADDRESSED

The relative gene and protein expression of CYP3A4 and CYP3A5 in human skin in comparison to liver remains unclear. It is also unknown if the expression is localized to the

dermis or epidermis and whether the enzymes are functionally active and are able to metabolise clinically relevant molecules.

3 EXPERIMENTAL DESIGN

See e-supporting information.

4 RESULTS

Gene expression levels of CYP3A4 and CYP3A5 were in much greater abundance in the liver than skin with expression being several hundred-fold greater for CYP3A4 and 9-fold for CYP3A5 respectively (Figure 1A-B). In human liver, gene expression of CYP3A4 was significantly greater ($p<0.001$) than for CYP3A5, whereas, in skin, gene expression of CYP3A5 was significantly greater ($p<0.001$) than that of CYP3A4 (Figure 1A-B). Immunoblot analysis revealed that both enzymes were also expressed at markedly lower levels in skin compared to liver (Figure. 1C-D), confirming the qPCR data. An immuno-positive band corresponding to CYP3A5 was not detected in skin at exposure times that were saturating for liver samples, however, when probed in isolation, CYP3A5 was detected when the exposure time was extended to increase assay sensitivity (Figure 1E). mRNA transcripts for CYP3A4 and CYP3A5 were detected in TESE. Gene expression levels for CYP3A4 were very low and several hundred-fold lower than for CYP3A5, and similar to native skin, TESE expressed significantly more mRNA transcripts for CYP3A5 than CYP3A4 ($p<0.001$) (Figure 1F), and significantly more CYP3A4 ($p<0.05$) and CYP3A5 ($p<0.01$) was expressed in the epidermis compared to the dermis (Figure 1G-H). Immunohistochemical analysis showed that CYP3A4 was equally distributed throughout the epidermis although absent in the cornified layers of both skin and TESE (Figure S1A-B). CYP3A4 staining was also observed in the majority of stromal fibroblasts and was prominent in the endothelium lining the blood vessels within the

connective tissue of native skin (Figure S1A). In contrast, staining was not observed in the fibroblasts populating the collagen hydrogel in the TESE (Figure S1B), supporting the qPCR data that showed very low mRNA expression in the TSE dermis. In native skin, expression of CYP3A5 was largely restricted to the stratum basale (Figure S2C) whereas expression in TESE models was extremely weak throughout the entire epithelium (Figure S1D). The discordant in immunostaining and qPCR data is likely due to low antibody affinity for CYP3A5. Both native skin and TESE revealed no staining in the dermis, suggesting that dermal fibroblasts do not express CYP3A5.

Liver extracts exhibited a maximal reaction velocity (V_{max}) of 6694 µmol/min/mg whilst native human skin extracts exhibited a lower V_{max} of 3215 µmol/min/mg. The V_{max} of TESE was approximately half that of native skin (1788 µmol/min/mg). Assuming that the enzyme catalytic rate (K_{cat}) for CYP3A for this substrate is the same in liver, skin and TESE, we can use these V_{max} estimates to calculate the relative tissue/extract enzyme expressions: namely, skin:liver=0.48:1; TESE:liver=0.267:1; TESE:skin=0.556:1 (Figure 2A-C).

Testosterone was applied to the stratum corneum or to the culture medium of TESE for 8 and 24 hours to mimic topical or systemic delivery. TESE models were separated into epidermal and dermal components and extracts of these along with the conditioned medium were analysed by mass spectrometry for presence of the CYP3A-generated metabolite, 6β-OH-testosterone. When testosterone was applied topically, 6β-OH-testosterone was detected in the epidermis, dermis and in the culture medium at both 8 and 24 hours. At 8 hours 6β-OH-testosterone levels were similar in the epidermis, dermis and medium whereas after 24 hours the levels of 6β-OH-testosterone found in the epidermis were markedly lower, levels in the dermis were similar, whereas levels in the

medium had increased five-fold compared to levels at 8 h ($p<0.001$)(Figure 2D). A markedly different pattern of metabolite production was observed when testosterone was added to mimic systemic delivery. In these models, the presence of 6β-OH-testosterone was not detected in the epidermal or dermal compartments at 8 or 24 hours, whereas after 8 hours, 6β-OH-testosterone was detected in the culture medium and these levels were significantly increased after 24 hours ($p<0.001$) (Figure 2E).

5 CONCLUSIONS

In this study we show both gene and protein expression of predominantly CYP3A5 but also CYP3A4 in native skin and TESE. These data have important clinical implications for dermal drug delivery of existing or new compounds, in particular those with structural components that are likely to be metabolised by CYP3A4/5. They also show that, although expressed at lower levels than skin, TESE are able to replicate the kinetics of skin metabolism of topically and systemically delivered drugs.

6 FUNDING

This study was funded by a National Centre for the Replacement, Refinement & Reduction of Animals in Research (NC3R) UK CRACK-IT Challenge 20 award.

7 CONFLICTS OF INTEREST

The authors have declared no conflicting interests.

8 AUTHOR CONTRIBUTIONS

SAS, HEC, KMS, RS-Y and PS performed the experiments and analysed the data. SDW and AS analysed the enzyme kinetic data. CM, SAS and HEC designed the research study and wrote the manuscript. CM and SDW supervised the research.

Keywords

Xenobiotic metabolism, Toxicity, Steroids, Three dimensional tissue models, Epithelium

9 REFERENCES

1. Guengerich F P. Common and uncommon cytochrome P450 reactions related to metabolism and chemical toxicity. *Chem Res Toxicol* 2001; 14: 611-650.
2. Palrasu M, Nagini S. Cytochrome P450 structure, function and clinical significance: A review. *Curr Drug Targets* 2017.
3. Guengerich F P. Cytochrome p450 and chemical toxicology. *Chem Res Toxicol* 2008; 21: 70-83.
4. Zanger U M, Schwab M. Cytochrome P450 enzymes in drug metabolism: regulation of gene expression, enzyme activities, and impact of genetic variation. *Pharmacol Ther* 2013; 138: 103-141.
5. Ohtsuki S, Schaefer O, Kawakami H, et al. Simultaneous absolute protein quantification of transporters, cytochromes P450, and UDP-glucuronosyltransferases as a novel approach for the characterization of individual human liver: comparison with mRNA levels and activities. *Drug Metab Dispos* 2012; 40: 83-92.
6. Flockhart D A, Rae J M. Cytochrome P450 3A pharmacogenetics: the road that needs traveled. *Pharmacogenomics J* 2003; 3: 3-5.
7. Williams J A, Ring B J, Cantrell V E, et al. Comparative metabolic capabilities of CYP3A4, CYP3A5, and CYP3A7. *Drug Metab Dispos* 2002; 30: 883-891.
8. Luu-The V, Duche D, Ferraris C, et al. Expression profiles of phases 1 and 2 metabolizing enzymes in human skin and the reconstructed skin models Episkin and full thickness model from Episkin. *J Steroid Biochem Mol Biol* 2009; 116: 178-186.
9. Wiegand C, Hewitt N J, Merk H F, et al. Dermal xenobiotic metabolism: a comparison between native human skin, four in vitro skin test systems and a liver system. *Skin Pharmacol Physiol* 2014; 27: 263-275.

10 LEGENDS FOR ILLUSTRATIONS

Figure 1. Comparison of gene and protein expression levels between human liver, skin and TESE for CYP3A4 and CYP3A5. cDNA from human liver and skin was subjected to qPCR analysis for CYP3A4 (blue) and CYP3A5 (red) and gene expression relative to GAPDH determined for (A) liver and (B) skin. Protein expression in liver and skin was resolved by immunoblotting for (C) CYP3A4 and (D) CYP3A5. (E) CYP3A5 expression in skin following prolonged exposure during infrared detection of immuno-positive bands; β-actin was used as a loading control and immunoblots are representative of 3 independent experiments. (F) Relative gene expression of CYP3A4 (blue) and CYP3A5 (red) in whole EpiDerm-FT400™ TESE by qPCR analysis. RNA from the epidermis and dermis of EpiDerm-FT400™ TESE was isolated, reverse transcribed and subjected to qPCR analysis for (G) CYP3A4 and (H) CYP3A5. Data are relative expression to GAPDH. Data are mean ± SD for n=3 independent experiments and 3 technical repeats per experiment. * P<0.05, ** P<0.01, ***p<0.001 by ANOVA.

Figure 2. Functional activity of CYP3A in liver, skin and TESE and testosterone metabolism by TESE. Protein extracts were generated from human liver, skin and EpiDerm-FT400™ TESE and subjected to kinetic enzyme analysis using increasing concentrations of the model substrate benzyl-*O*-methyl-cyanocoumarin (BOMCC). A Nelder-Mead algorithm was used to fit the enzyme activity data and all data sets were fit with the assumption that K_m (the binding affinity for the substrate at half the maximum velocity) was the same in each assay (K_m = 10 µM). Maximum velocity (V_{max}) was calculated as specific metabolic activity of CYP3A in µmol/min/mg. Data are from three independent experiments performed in triplicate. Goodness of fit R^2 values are: (A) 0.8855, (B) 0.9779 and (C) 0.9962**.** Testosterone

was added either to (C) the surface of the epidermis to mimic topical drug deliver or (D) added to the medium that bathes the dermis to mimic systemic drug delivery. The production of the specific testosterone metabolite 6β-OH-testosterone was measured by mass spectrometry in epidermal and dermal extracts as well as the tissue culture medium after 8 and 24 h. Data are from 2 independent experiments and 3 technical repeats per experiment.

Supplementary Figure 1. Spatial localisation of metabolising enzyme expression in native skin and TESE. Formalin-fixed, paraffin-embedded sections of native human skin and EpiDerm-FT400™ TESE were analysed by immunohistochemistry to determine the spatial expression of CYP3A4 (A & B) and CYP3A5 (C & D). IgG was used as a control (E & F). Scale bar =100 µm. Images are representative of 3 independent experiments from 3 different tissues.

Experimental design

2.1 Tissue engineered skin equivalents (TESE)

EpiDermFT-400™ TESE comprising of a stratified squamous epithelium composed of differentiating skin keratinocytes cultured on top of a dermal fibroblast-populated collagen hydrogel were purchased from MatTek Corporation (Ashland, MA, USA). Upon receipt EpiDermFT-400™ TESE were transferred to 6 well plates and incubated overnight at 37°C, 5% CO_2 in a modified flavin- and adenine- enriched medium consisting of: DMEM and Ham's F12 medium in a 3:1 (v/v) ratio supplemented with 10% (v/v) fetal calf serum (FCS), 0.1 mM cholera toxin, 10 ng/ml epidermal growth factor, 0.18 mM adenine, 5 µg/ml insulin, 5 µg/ml transferrin, 2 mM glutamine, 0.2 mM triiodothyronine, 0.625 mg/ml amphotericin B, 100 IU/ml penicillin and 100 mg/ml streptomycin (all Sigma, Poole, UK).[S6]

2.2 RNA and protein extraction

Whole TESE, or separated epithelial and dermal layers from EpiDermFT-400™ TESE were homogenized to ensure complete lysis and total RNA extracted using the RNAeasy mini kit (Qiagen, Hilden, Germany). For protein lysis, all samples were snap frozen with liquid nitrogen, homogenized with a pestle and mortar, transferred to lysis buffer (50 mM Tris, 150 mM NaCl, 1% Triton-X-100, pH 7.6) and aspirated through a 25-gauge needle before incubation on ice for 20 minutes. Samples were then centrifuged at 15,000 x g for 20 minutes with the resulting supernatants removed and stored at -80°C. Protein levels were determined using a bicinchoninic acid protein assay (ThermoFisher Scientific, MA, USA).

2.3 Quantitative real-time PCR analysis

One µg of human liver total RNA (Amsbio, Abingdon, UK), human skin total RNA (Amsbio, Abingdon, UK) or EpiDermFT-400™ TESE total RNA was reversed transcribed to cDNA using High Capacity Reverse Transcription kit (Applied Biosystems, CA, USA) according to the manufacturer's instructions. Quantitative real-time polymerase chain reaction (PCR) was performed in a 10 µl reaction volume using 1 µl of cDNA, along with Taqman MGB human FAM-labelled probes CYP3A4 (Hs00604506_m1), CYP3A5 (Hs01070905_m1) and GAPDH (Hs02758991_g1) (ThermoFisher) and Taqman Mastermix, and the reaction carried out in a 7900HT Fast Real-Time PCR System (Applied Biosystems, CA, USA). Critical threshold (ct) and ΔCt values were calculated for each sample and relative expression of target genes, normalized to the abundance of the reference control transcript (GAPDH) calculated. For certain analysis, the relative fold change in gene expression was calculated using the formula $2^{-\Delta\Delta Ct}$.

2.4 Immunoblotting

Thirty µg of human liver tissue lysate (Abcam, Cambridge, UK) or human skin tissue lysate (Abcam) were separated by SDS-PAGE (4-12%) and transferred to nitrocellulose membranes (Bio-Rad, Watford, UK). Membranes were blocked for 1 hour in 5% TBST (5% milk powder, Tris-buffered Saline, 0.1% Tween-20) at room temperature. Membranes were incubated at 4°C overnight with primary antiserum directed against CYP3A4 (1:200, EPR6202, Abcam), CYP3A5 (1:500, EPR4396, Abcam) or β-actin (1:3000, Abcam) diluted in 5% TBST. After washing in TBST, membranes were incubated for 1 hour in 5% TBST with either IRDye

800CW donkey anti-rabbit (1:10,000, 926-32213, LI-COR Biosciences) or IRDye 680RD donkey anti-goat (1:10,000, 926-68074, LI-COR Biosciences) antiserum. Membranes were washed an additional three times with TBST prior to development using LI-COR Odyssey system (LI-COR Biosciences).

2.5 Immunohistochemistry

Formalin-fixed, paraffin-embedded native skin obtained with informed, written consent from patients undergoing maxillofacial surgery (ethical approval 09/H1308/66) or EpiDermFT-400™ TESE were sectioned (5 µm) and mounted on adhesive glass slides (Leica Biosystems, Wetzlar, Germany). Antigen retrieval was performed using citrate buffer (10 mM sodium citrate, 0.05 % Tween-20, pH 6.0, 20 min, 95°C) or Tris buffer (10 mM Tris Base, 0.05% Tween-20, pH 10) in a 2100 Antigen Retriever (Aptum Biologics Ltd, Hampshire, UK). Sections were blocked for 30 minutes at room temperature using serum-free protein block (Dako-Agilent Technologies, CA, USA) for 20 minutes and then incubated for 1 hour with primary antibody directed to CYP3A4 (1:250, ab3572, Abcam), CYP3A5 (1:250, ab108624, Abcam); IgG was used as a non-specific control. Following washing with PBS, sections were incubated with a biotinylated secondary antibody for one hour, followed by a 30 minute incubation with an avidin-biotin complex kit (Vectastatin Elite ABC kit, Vector Laboratories, Peterborough, UK) and antigens visualized using 30-diaminobenzidine tetrahydrochloride (DAB) (Vector Labs), according to the manufacturer's instructions. Nuclei were counterstained with haematoxylin, and sections then dehydrated and mounted in DPX. Images were taken using an Olympus BX51 microscope and Colour view IIIu camera with associated Cell^D software (Olympus Soft Imaging Solutions GmbH, Münster, Germany).

2.6 CYP3A kinetic assay

The commercially available Vivid® CYP450 Blue Screening Kit (ThermoFisher Scientific, MA, USA) was modified to assess functional activity following CYP3A biotransformation of benzyl-*O*-methyl-cyanocoumarin (BOMCC). Forty µl of liver, skin or EpiDermFT-400™ cell lysate and 50 µl of master mix (49 µl of 1 x reaction buffer, 1 µl of regeneration system) was added to each well of a 96-well plate and the plate was incubated at room temperature for 10 minutes. 10 µl of substrate mix was added to each well (1 x reaction buffer, Vivid® NADP+, and desired concentration of Vivid® BOMCC substrate) and readings taken at excitation wavelength 415 nm and emission wavelength 460 nm at 10-minute intervals for a total of 120 minutes using a Tecan spectrophotometer. Concentrations were interpolated from a standard curve generated using standards provided with kit. A Nelder-Mead fitting algorithm within Matlab (MathsWorks Inc.) was used to fit the enzyme activity data to Michaelis-Menten kinetic curves (of the form, $v_0=V_{max}$ [BOMCC]/(K_m+[BOMCC]), where K_m (mM) is the Michaelis-Menten enzyme-substrate affinity constant and V_{max} = K_{cat}[CYP3] (µmol/min/mg) is the maximum enzyme activity rate, where K_{cat} (1/min) is the turnover catalytic rate and [CYP3] (µmol/mg) is the total CYP3 expression and [BOMCC] is the concentration of substrate (µM). Coefficient of determination (R^2) is used as a determinant of goodness of fit in each case. All data sets were independently fit with the assumption that the binding affinity K_m value was the same for each assay (K_m for BOMCC = 10 µM (data provided by ThermoFisher Scientific) - under the assumption that CYP3:BOMCC interactions occurred with the same affinity in each case). Enzyme expression fold changes were

obtained by calculating the ratio of V_{max} values under the assumption that the turnover catalytic rate (K_{cat}) was also the same in each assay.

2.7 Mass Spectrometry

EpiDermFT-400™ TESE were transferred to 6-well plates and incubated overnight at 37°C, 5% CO_2 in a modified flavin- and adenine- enriched medium. TESE were treated with 1 mM testosterone (Sigma, Poole, UK) in phenol red-free medium for 8 and 24 hours, either to the surface of the model (to mimic topical delivery) or within the culture medium (to mimic systemic delivery). The epidermal and dermal layers were separated using forceps and each placed into 2 ml of phenol red-free medium before being snap frozen and stored in liquid nitrogen. Testosterone analysis was carried out as previously described.[S7] In brief, samples were analysed using a quadrupole linear ion trap mass spectrometer (AB Sciex 4000 QTrap) coupled to a Dionex Ultimate 3000 HPLC system. 10 µL of each sample was separated using a Phenomenex Luna 5 µ C18(2) 100A 100 x 2.00 mm column and a gradient consisting of 0.1 % formic acid in water (mobile phase A) and methanol (mobile phase B) with a 200 mL/minute flow rate. The column oven and auto-sampler were maintained at 30°C and 4°C respectively. The mass spectrometer was operated using the multiple reaction monitoring mode and the analytes detected and quantified using the most abundant transitions obtained during direct infusion of commercially available LC-MS-MS grade standard.

2.8 Statistical Analysis

All data presented are from at least 3 independent experiments unless stated otherwise and results expressed as mean ± standard deviation (SD). Differences between groups were

measured using Student's t-test calculated in Graphpad Prism v6.0 (GraphPad, La Jolla, CA) and statistical significance was assumed if $p<0.05$.

S1. Yengi L G, Xiang Q, Pan J, et al. Quantitation of cytochrome P450 mRNA levels in human skin. *Anal Biochem* 2003; 316: 103-110.

S2. Saeki M, Saito Y, Nagano M, et al. mRNA expression of multiple cytochrome p450 isozymes in four types of cultured skin cells. *International archives of allergy and immunology* 2002; 127: 333-336.

S3. Hu T, Khambatta Z S, Hayden P J, et al. Xenobiotic metabolism gene expression in the EpiDermin vitro 3D human epidermis model compared to human skin. *Toxicol In Vitro* 2010; 24: 1450-1463.

S4. van Eijl S, Zhu Z, Cupitt J, et al. Elucidation of xenobiotic metabolism pathways in human skin and human skin models by proteomic profiling. *PLoS One* 2012; 7: e41721.

S5. Hewitt N J, Edwards R J, Fritsche E, et al. Use of human in vitro skin models for accurate and ethical risk assessment: metabolic considerations. *Toxicol Sci* 2013; 133: 209-217.

S6. Allen-Hoffmann B L, Rheinwald J G. Polycyclic aromatic hydrocarbon mutagenesis of human epidermal keratinocytes in culture. *Proc Natl Acad Sci U S A* 1984; 81: 7802-7806.

S7. Baxter M, Withey S, Harrison S, et al. Phenotypic and functional analyses show stem cell-derived hepatocyte-like cells better mimic fetal rather than adult hepatocytes. *J Hepatol* 2015; 62: 581-589.

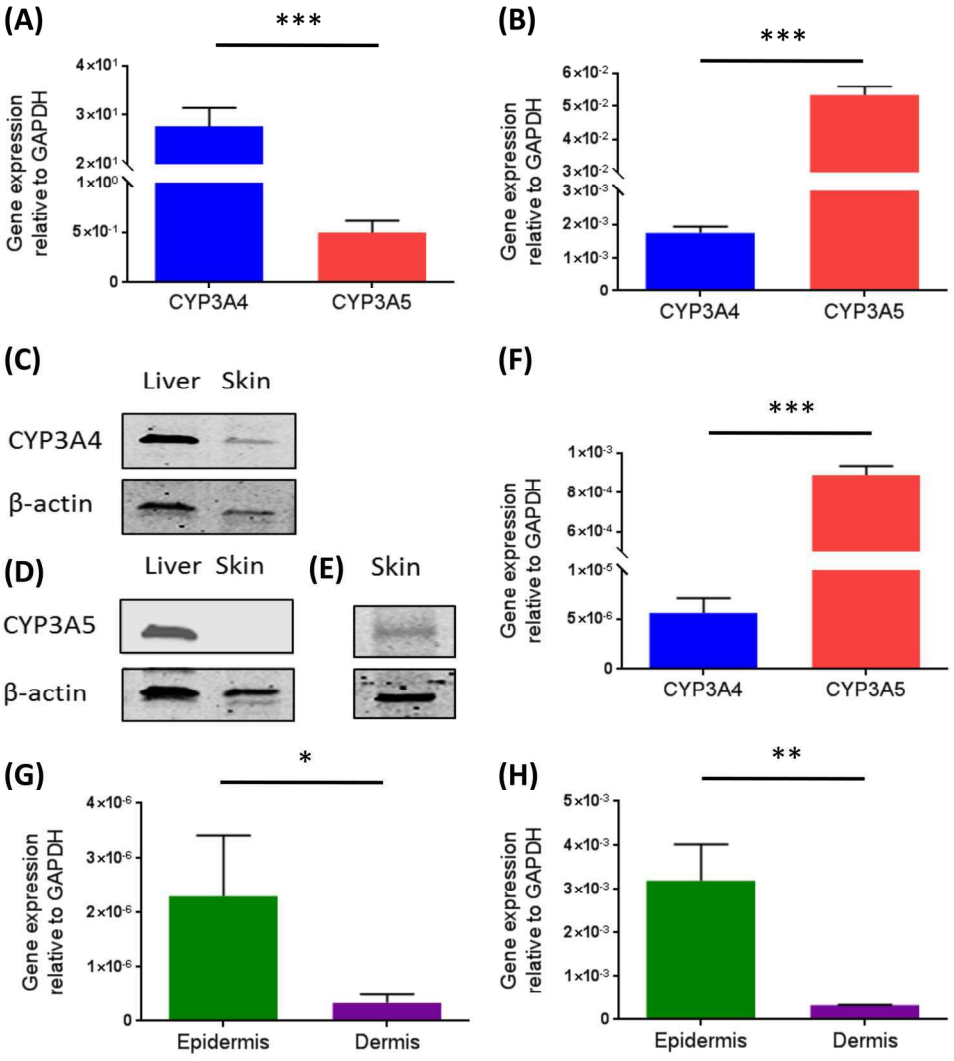

Figure 1. Comparison of gene and protein expression levels between human liver, skin and TESE for CYP3A4 and CYP3A5. cDNA from human liver and skin was subjected to qPCR analysis for CYP3A4 (blue) and CYP3A5 (red) and gene expression relative to GAPDH determined for (A) liver and (B) skin. Protein expression in liver and skin was resolved by immunoblotting for (C) CYP3A4 and (D) CYP3A5. (E) CYP3A5 expression in skin following prolonged exposure during infrared detection of immuno-positive bands; β-actin was used as a loading control and immunoblots are representative of 3 independent experiments. (F) Relative gene expression of CYP3A4 (blue) and CYP3A5 (red) in whole EpiDerm-FT400™ TESE by qPCR analysis. RNA from the epidermis and dermis of EpiDerm-FT400™ TESE was isolated, reverse transcribed and subjected to qPCR analysis for (G) CYP3A4 and (H) CYP3A5. Data are relative expression to GAPDH. Data are mean ± SD for n=3 independent experiments and 3 technical repeats per experiment. * P<0.05, ** P<0.01, ***p<0.001 by ANOVA.

88x97mm (600 x 600 DPI)

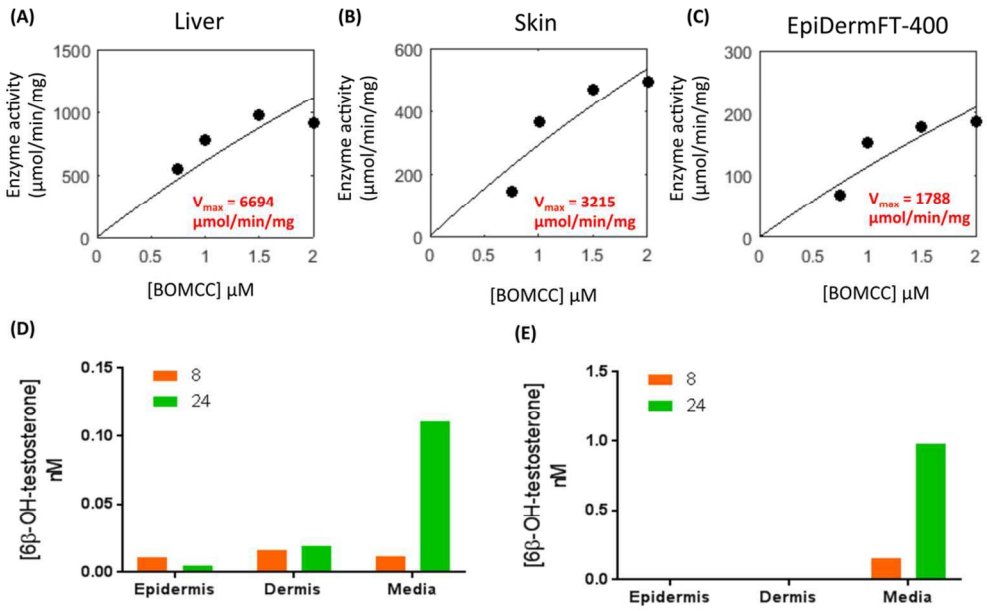

Figure 2. Functional activity of CYP3A in liver, skin and TESE and testosterone metabolism by TESE. Protein extracts were generated from human liver, skin and EpiDerm-FT400™ TESE and subjected to kinetic enzyme analysis using increasing concentrations of the model substrate benzyl-O-methyl-cyanocoumarin (BOMCC). A Nelder-Mead algorithm was used to fit the enzyme activity data and all data sets were fit with the assumption that Km (the binding affinity for the substrate at half the maximum velocity) was the same in each assay (Km = 10 µM). Maximum velocity (Vmax) was calculated as specific metabolic activity of CYP3A in µmol/min/mg. Data are from three independent experiments performed in triplicate. Goodness of fit R2 values are: (A) 0.8855, (B) 0.9779 and (C) 0.9962. Testosterone was added either to (C) the surface of the epidermis to mimic topical drug deliver or (D) added to the medium that bathes the dermis to mimic systemic drug delivery. The production of the specific testosterone metabolite 6β-OH-testosterone was measured by mass spectrometry in epidermal and dermal extracts as well as the tissue culture medium after 8 and 24 h. Data are from 2 independent experiments and 3 technical repeats per experiment.

49x31mm (600 x 600 DPI)

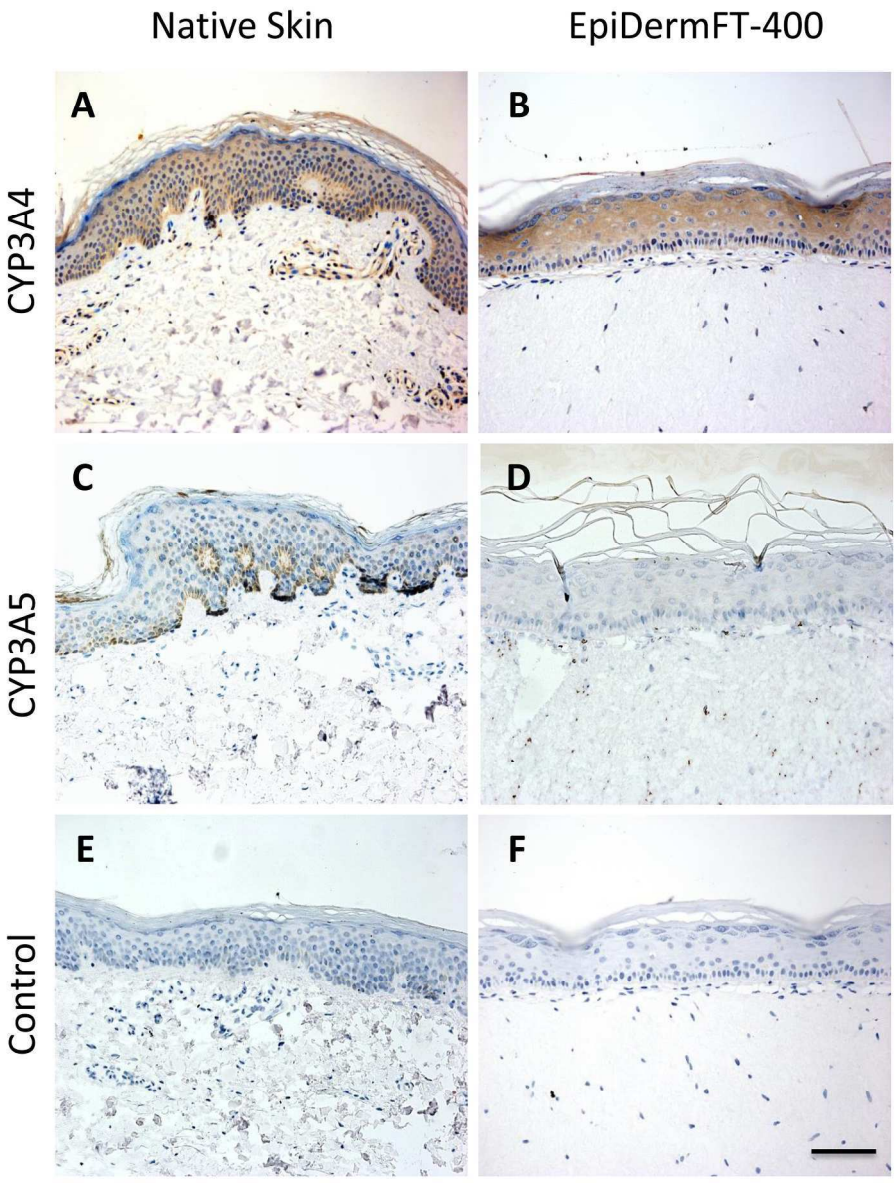

101x128mm (600 x 600 DPI)